2009

Material Selection of Z-fibre in Stitched Composites - Experimental and Analytical Comparison Approach

Kwek Tze Tan
University of Akron Main Campus

N. Watanabe

M. Sano

M. Takase

Y. Iwahori

See next page for additional authors

Authors
Kwek Tze Tan, N. Watanabe, M. Sano, M. Takase, Y. Iwahori, and H. Hoshi

MATERIAL SELECTION OF Z-FIBRE IN STITCHED COMPOSITES – EXPERIMENTAL AND ANALYTICAL COMPARISON APPROACH

K.T. Tan*, N. Watanabe*, M. Sano*, M. Takase*, Y. Iwahori** and H. Hoshi**
*Department of Aerospace Engineering, Tokyo Metropolitan University
**Japan Aerospace Exploration Agency
6-6 Asahigaoka, Hino, Tokyo 191-0065, Japan
tan-kwektze@sd.tmu.ac.jp

SUMMARY

Strain energy release rates are measured and compared for laminated composites stitched with different fibre materials – Carbon, Kevlar and Vectran. DCB test and FE simulation are performed to evaluate the interlaminar toughness. It is proven that Vectran provides the toughest interlaminar reinforcement and is most suitable for Z-fibre application.

Keywords: Stitched Composites, Interlaminar Toughness, Vectran, Kevlar, Z-fibre, Carbon

INTRODUCTION

There has been a vast amount of research work dedicated to stitched composites over these years [1-8]. This is inspired by the need to effectively improve the generally poor interlaminar strength of laminated composites. In stitched composites, stitch fibres offer resistance to delamination crack propagation. This is because during interlaminar mode I fracture propagation, the stitch fibres undergo tensile breakage and thus additional energy is required to break the stitch fibres. Experimental and computational analyses on stitched composites recorded in scientific literatures are normally performed using either Kevlar or Carbon as Z-fibre stitches. Kevlar is generally more preferred than Carbon fibres, as Carbon fibres make bending difficult in stitching process due to its very high stiffness. However, Kevlar has a great disadvantage because of its high moisture absorption, which could result in in-plane swelling during application. Vectran®, a relatively new fibre material, having comparable properties with Kevlar, is more superior due to its very low moisture absorption. Table 1 shows the comparison of properties between Vectran, Kevlar and Carbon fibres.

Table 1. Comparison of Properties of Various Yarn Materials

Material	Density (g/cm^3)	Tensile Strength (GPa)	Tensile Modulus (GPa)	Moisture Regain	Yarn Elongation (%)
Vectran HT	1.41	3.2	75	<0.1	3.3
Carbon TR-40	1.80	3.1	221	-	1.4
Kevlar-29	1.44	2.9	71	3.7	3.6

The role of stitched composites, with a reinforced interlaminar strength, has extended to many areas of application where stringent design requirements on chemical and moisture resistance are required. There are many kinds of yarn materials available for Z-fibre stitching; however, there is currently no report on material performance comparison of Z-fibre, which limits the fibre selection of stitched composites in further practical application.

This paper presents both an experimental and analytical comparison approach by investigating the interlaminar fracture toughness of laminated composites stitched by Carbon, Kevlar and Vectran fibres. Double Cantilever Beam (DCB) tests were carried out on various stitch densities (SD) and thread thicknesses of Carbon, Kevlar and Vectran stitched CFRP laminates. The results, including Load-Crack Opening Displacement (COD) curves and R-curves, are validated using Finite Element Analysis (FEA) simulation, based on the FE stitch model which simplifies the complex nature of stitch fracture into four progressive steps: firstly, interfacial debonding between Z-fibre and regional matrix; secondly, slack absorption of Z-fibre; thirdly, fibre breakage of Z-fibre and lastly, frictional effect during pull-out of Z-fibre. The linear relationship of G_I-SD and G_I-V_{ft} plots for Carbon, Kevlar and Vectran stitched laminates are presented and insights on the difference between Kevlar and Vectran stitch fracture behaviour, provided by Interlaminar Tension Test (ITT), are discussed.

EXPERIMENTAL WORK

Material Preparation

The specimens were made of Carbon Fibre Reinforced Polymer (CFRP) 24-ply quasi-isotropic $[+45/0/-45/90]_{3S}$ laminates of Toray Industries T700GC-12K, stitched in through-thickness direction using Vectran, Kevlar or Carbon fibres. The linear density of Vectran single yarn threads used is 200denier and 500denier, while that for Kevlar is 400denier and 600denier. Carbon single yarn fibres are of 610denier. Stitch densities of the specimens are varied by having different stitch pitch (distance between two adjacent stitches in the same row) and stitch space (spacing between two adjacent stitch rows). The type of stitch used in this study is the Modified Lock stitch. It is worth noting that each stitch consists of two yarn fibres. After the stitching process, resin transfer moulding technique, at a curing temperature of 180°C, was adopted to consolidate the composite. The resin used in this case is Araldite LY564.

DCB Tests Procedure

Unidirectional CFRP laminates of thickness 2mm were secondarily bonded to both sides of DCB test specimens by using the film adhesive to create a tabbed DCB configuration. This is to prevent premature fracture due to high bending moment stress incurred by flexure during DCB test. A cut-out of 2mm thickness and length 25mm, tapered to 1mm thickness and length 5mm was machined, using a diamond wheel fine cutter, into the specimen, for insertion of a steel loading fixture. An initial crack length of 5mm was given to the specimen with a very sharp razor. The configuration and dimensions of the specimen are shown in Figure 1. The DCB specimen was tested with an INSTRON 5500R screw-driven testing machine in displacement-controlled mode at a crosshead speed of 0.5mm/min. Experimental Setup for the DCB test can be seen in Figure 2. During the experiment, the specimen was loaded until the sudden load drop, and the machine was stopped to measure the crack length using markers along the length of the specimen. The crack length was determined by averaging the values on both sides of the specimen. This procedure was repeated at each load drop.

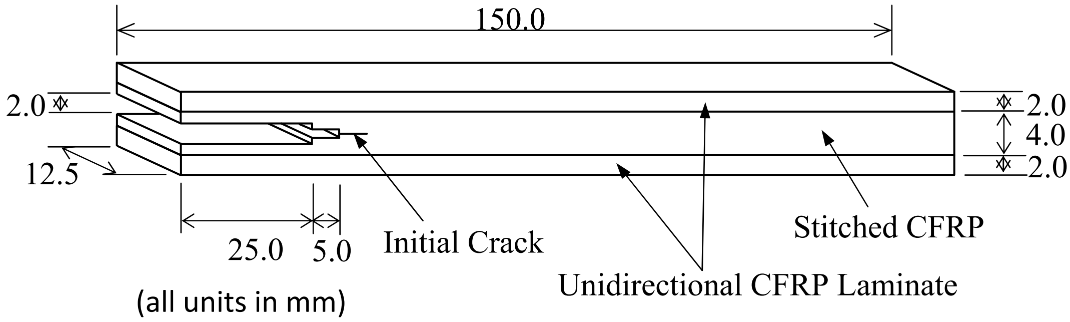

Figure 1. Tabbed DCB Test Specimen

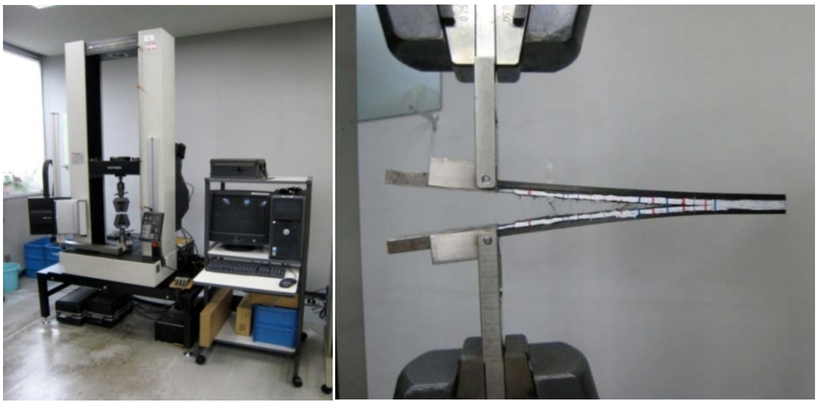

Figure 2. DCB Test: INSTRON Machine (left); DCB specimen under testing (right)

From the Load-COD graphs and crack length measurements, Mode I Interlaminar Fracture Toughness (G_I) was calculated based on the commonly used *area method* given in Equation (1). This method is a direct energy measurement and is very popular because of its simplicity.

$$G_I = \frac{\Delta A_{ij}}{w(a_j - a_i)} \tag{1}$$

where, ΔA_{ij} is the area under load-displacement curve between crack lengths a_j and a_i and w is the specimen width.

Interlaminar Tension Test Material Preparation and Procedure

Interlaminar Tension Test (ITT) is a novel test method to understand the mechanical progressive damage behaviour of a single Z-fibre stitch thread undergoing a tensile force [7 & 8]. The results of this test are expected to provide a better physical understanding of the mechanics and mechanisms of Z-fibre stitching. A single stitch thread was isolated to within 5mm by 5mm area of the 15mm by 15mm composite test specimen. The specimen dimensions and experimental setup are depicted in Figure 3. The test piece was then bonded to aluminium T-Shaped Jig Frame by epoxy adhesive. A uniaxial tensile test was performed until the stitch thread was broken and pulled out completely. The crosshead speed was 0.25mm/min and measurements of the load and displacement were taken.

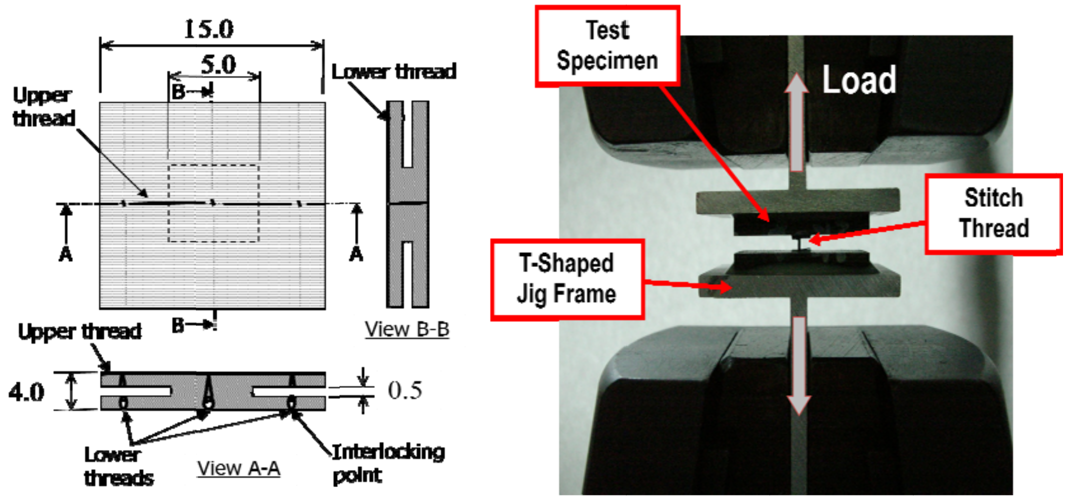

Figure 3. ITT: Specimen Dimensions (left); Experimental Setup (right)

FEM SIMULATION ANALYSIS

FE Composite Laminate Model

FEM simulation is developed to model the interlaminar fracture phenomenon of stitched CFRP laminates as experienced in DCB test, integrating the primary idea of fracture process in the Z-fibre vicinity. The numerical model used is based on a 2-D FEM model developed earlier [4]. This 2-D model assumes a plane stress condition and the crack front propagates straight along the x-direction of the model. The FE simulation models the CFRP 24-ply quasi-isotropic $[+45/0/-45/90]_{3S}$ laminates as the same layup as the DCB test specimens. However, only half the laminate is modelled due to the case of symmetry, and each in-plane CFRP composite stack lay-up, [+45/0/-45/90], is homogenised into one orthotropic layer. The equivalent elastic constants of the orthotropic layer and that of the unidirectional CFRP tab are summarised in Table 2, as in the case of Vectran-stitch analysis. The model includes the initial crack length, a_0, of 5mm measured from the point of loading, and the initial cut-out slot of 30mm for steel loading fixture. The FE mesh for the tabbed DCB model is illustrated in Figure 4.

Table 2. Mechanical Constants used in FE Simulation

Elastic Properties	E_x (GPa)	E_z (GPa)	G_{xz} (GPa)	ν_{xz}
CFRP Composite Stack	51.17	5.8	3.7	0.38
Unidirectional CFRP Tab	118.00	8.0	3.7	0.32

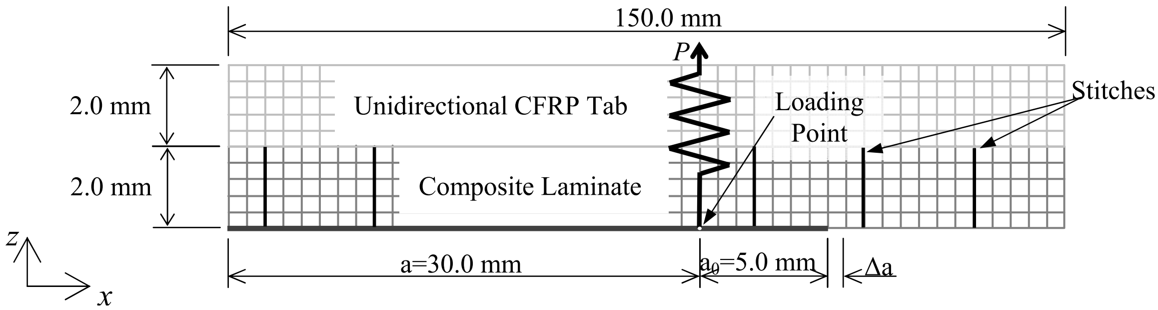

Figure 4. Finite Element Model of Tabbed DCB Test Specimen

An 8-noded isoparametric rectangular element is used in the modelling for both the composite laminate layer, as well as the unidirectional CFRP tab. The adhesive layer between the composite and tab is assumed negligible and ignored in the simulation. The crack length increment, Δa, is taken to be the same as the element unit length of 0.5mm. The effects of the loading fixture are modelled by an equivalent spring element. G_I was similarly calculated by the area method at each iteration step and the crack was deemed to extend virtually if G_I exceeds G_{IC}, which is assumed to increase linearly from 0.3 J/m^2 to 0.6 J/m^2 once crack length becomes 50mm for all stitch cases. The FEM simulation was executed until the crack length reached 100mm from the initial crack tip.

FE Stitch Model

The Z-fibre stitch is modelled as a 3-noded rod element with constant cross sectional area and axial stiffness. The stitch element assumes a series of progressive behaviour governed by the effect of its nodal forces to determine its damage condition and failure state. The initial stitch condition is perfectly bonded to its regional matrix, with a presumably small amount of slack. The model assumes that the stitch cannot be totally "slack free", considering the high-stiffness of the Z-fibre and the limitation of stitch tension by the stitching process. The fibre slack contributed to the bridging effect by providing a longer bridging zone. As the crack front approaches during interlaminar fracture, interfacial debonding occurs between the fibre and matrix when the stitch nodal force exceeds the debonding strength. Immediately after debonding, slack absorption occurs, as the stitch fibre continues to bridge across the crack, and is deemed to be completed when the extension exceeds the slack absorption value. The Z-fibre is considered to have fractured when the stitch nodal force reaches the fibre breakage strength. During pull-out of the fibre, frictional force provides the closure effect against the crack opening. The entire stitch failure process is completed once the stitch nodal displacement reaches the final pull-out distance, representing a complete pull-out of the Z-fibre. The entire stitch fracture process is summarised schematically in Figure 5.

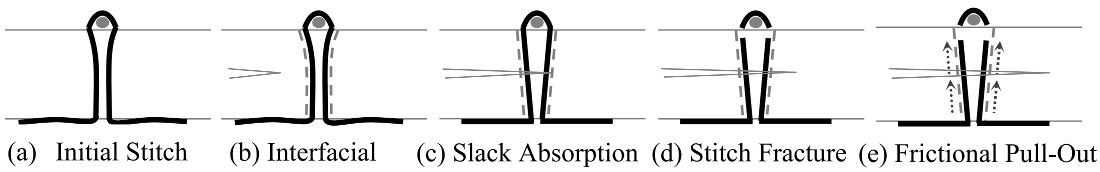

Figure 5. Progressive Damage of Stitch Fracture

RESULTS AND DISCUSSIONS

DCB Experiment - FE Simulation Correlation

DCB experimental results are validated using FE simulation. The critical input parameters for the FE model, such as debonding strength, fibre fracture strength, frictional pull-out force and final pull-out displacements, which characterised the stitch damage model, are obtained from a series of ITT results. Slack absorption values are calculated by separate stress-strain plots based on the ITT load-displacement curves and modulus of the stitch fibre. Typical ITT results for Vectran stitch fibre are shown in Figure 6. The first sharp peak load, resulted from the parent composite laminate fracture, is ignored and removed from the averaged graph, as the real focus of this study is on the mechanics and damage progression of the Z-fibre.

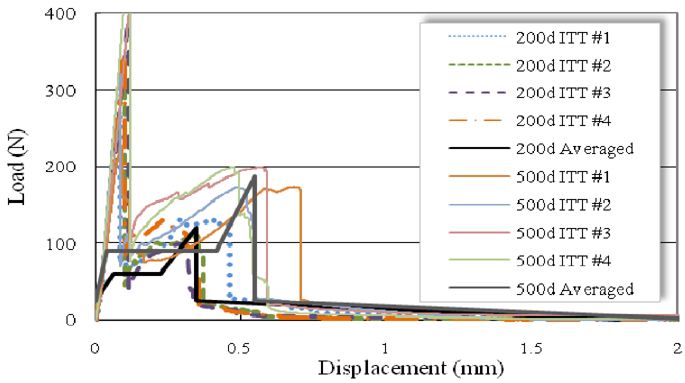

Figure 6. ITT Results of Vectran Single Fibre

Typical DCB load-COD results, both experimental and computational, for Vectran 200d and 500d, with different stitch densities are shown in Figure 7. The overall curve pattern and the descending load part of the experimental data and simulation result shows good correlation. Typical 'saw-edged' curve pattern for stitched laminates is evident. This characteristic is due to load drop as a result of progressive fracture of Z-fibres during crack propagation. Smaller and closer load drops are observed in denser stitch configuration. The FE model has predicted reasonably correct load peaks for all cases.

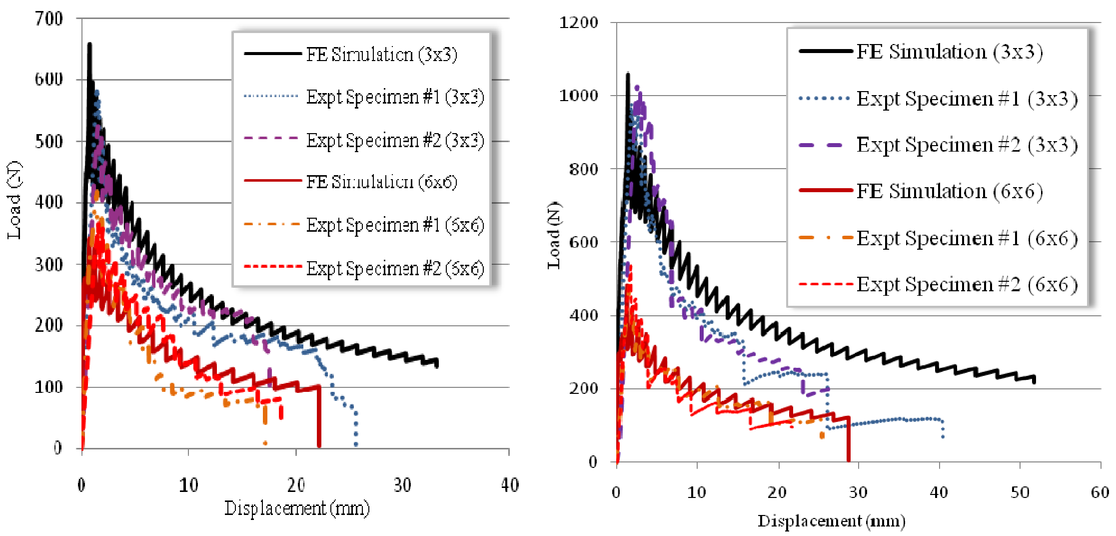

Figure 7. DCB Test Results for Vectran 200d (left) and 500d (right)

Corresponding R-curves for Vectran stitched composites are presented in Figure 8. The R-curves for all cases show good agreement with experimental data. It is demonstrated that fracture toughness increase with increasing thread thickness and increasing stitch density. The fracture toughness could be improved by 2 times from a moderately stitched to a densely stitched configuration in Vectran 200d and up to 3 times for that in Vectran 500d. These results verify the accuracy of the experimental G_I measurements, as well as the validity of the FE stitch model and its G_I prediction. Interlaminar fracture toughness of Kevlar and Carbon stitched laminates are similarly calculated by verifying experimental data with FE results. The next section presents the comparison summary.

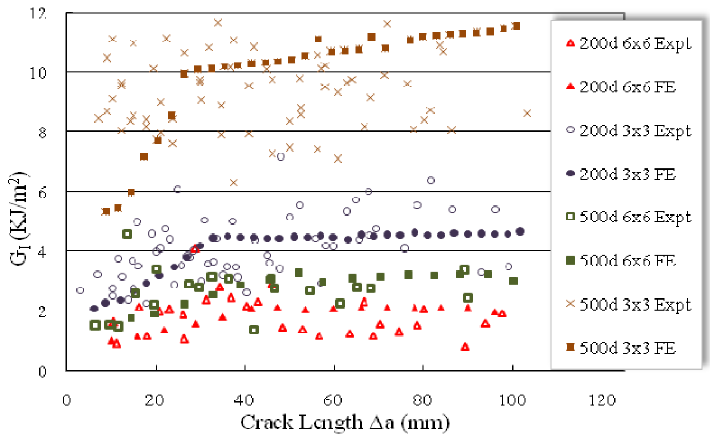

Figure 8. R-Curves for Vectran Stitched Composites

Interlaminar Strengthening Effect of Different Stitch Fibre Material

The results of G_I against SD, where SD is the stitch density, using linear regression method, for Carbon, Kevlar and Vectran stitched laminates are plotted in Figure 9. Linear relationship of G_I-SD is revealed and this linear relationship is true for all stitch materials and thread thicknesses. This information is useful to obtain new G_I value (given a different SD parameter) by extrapolation without executing further tests. These results further indicate that interlaminar strengthening effect increases with increasing thread thickness, as well as with increasing SD. Vectran thread 500d is compared with CF thread 610d and Kevlar thread 600d – both of comparable thicknesses. Vectran 500d shows the highest G_I /SD ratio value of about 50% more than Kevlar and CF. Vectran 200d, despite having thinner thread thickness than Kevlar 400d, shows almost equivalent G_I-SD relationship as Kevlar 400d. It is also worth noting that, for both Vectran and Kevlar, the material thickness is approximately directly proportional to the G_I /SD ratio value.

A further plot of G_I against V_{ft} (V_{ft} being the Z-fibre volume fraction) in Figure 10 confirms the G_I –fibre volume fraction linear relationship for Vectran, Kevlar and Carbon stitch fibre, irrespective of stitch thread thickness. Equivalent G_I/V_{ft} ratio is noted for the same fibre material. The G_I/V_{ft} comparison clearly reveals that Vectran stitch fibre is more effective in interlaminar strengthening by exhibiting a G_I/V_{ft} value 60% higher than Kevlar and Carbon. This result concludes that Vectran is a better material choice for Z-fibre application.

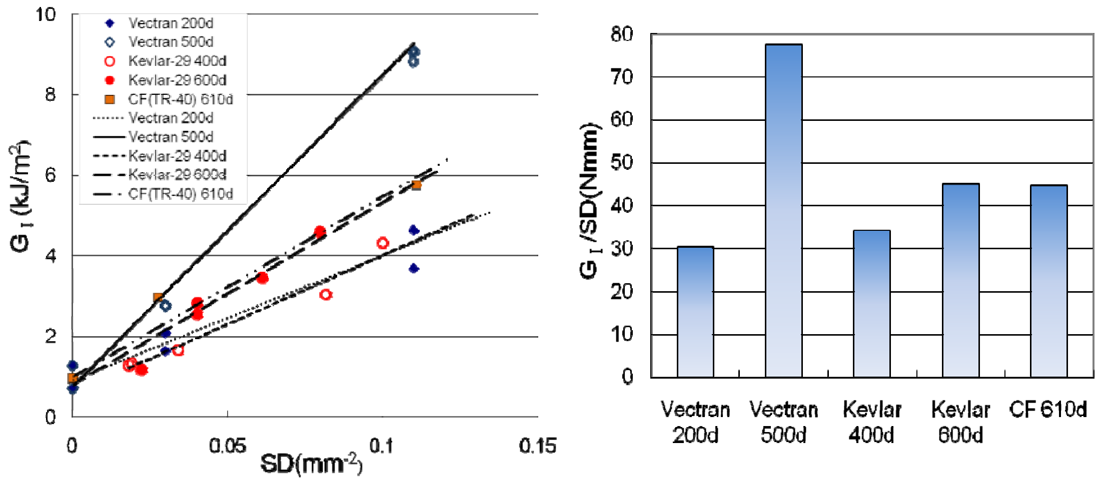

Figure 9. Effects of Z-Fibre Materials on G_I against Stitch Density (left); G_I/SD Comparison between Vectran, Kevlar and Carbon (right)

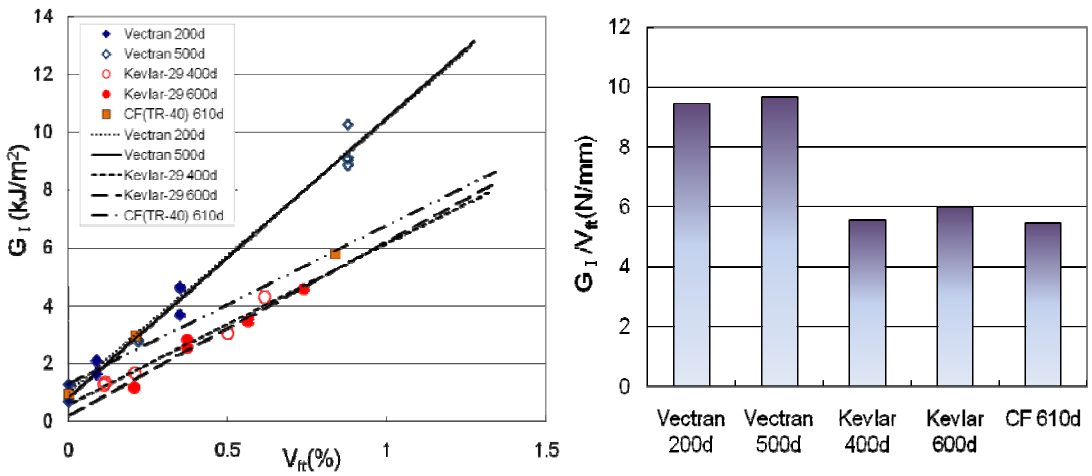

Figure 10. Effects of Z-Fibre Materials on G_I against Fibre Volume Fraction (left); G_I/V_{ft} Comparison between Vectran, Kevlar and Carbon (right)

Characterising Fracture Behaviour of Single Kevlar and Vectran Stitch

This section provides insights on the difference between Kevlar and Vectran stitch fracture behaviour, by examining experimental ITT results and FE slack absorption values. Figure 11 shows the ITT results comparison of single Kevlar and Vectran stitch fibre. It is noted that both Vectran 500d and Kevlar 600d fracture around the same breaking load of 200N. However, Vectran 500d breaks at a higher displacement of around 0.6mm, compared to that of Kevlar 600d at around 0.3mm. This displacement difference creates a vast disparity in total strain energy of about more than 2 times. It is clear that the difference in strain energy required for fibre breakage accounts for the difference in interlaminar fracture toughness of Vectran and Kevlar stitched composites. Both Vectran 200d and Kevlar 400d also indicate similar fibre breaking load of about 120N, and analogous to the thicker threads, Vectran 200d breaks at a displacement higher than Kevlar 400d, which results in a higher strain energy consumption. It should be mentioned that the strain energy consumption is solely based on fibre breakage and the slight discrepancy in the initial parent composite fracture is disregarded. Based on the same original length and almost equivalent tensile modulus of Kevlar and Vectran (Table 1), this displacement difference when translates into strain difference, results in different slack absorption values used in Vectran and Kevlar FE simulation. In the FE analysis, the slack absorption value used for Vectran 500d is 9.5%, whereas that of Kevlar 600d is 5%. Considering almost similar fibre breaking strength and Young modulus, the Vectran 500d model captured the higher slack absorption value and calculates a larger strain energy release rate, due to more substantial bridging effect by providing a longer bridging zone. The slack absorption value calculated for Vectran 200d and Kevlar 400d is 4% and 2.5% respectively. Figure 12 illustrates the importance of correct slack absorption value, using Vectran 500d 6x6 as an example. In this case, the 9.5% model simulates the experimental results most accurately. Based on Load-COD curves and R-curves, FE simulation validates the accuracy of the slack absorption value calculated from stress-strain plots for all thread thicknesses and fibre materials.

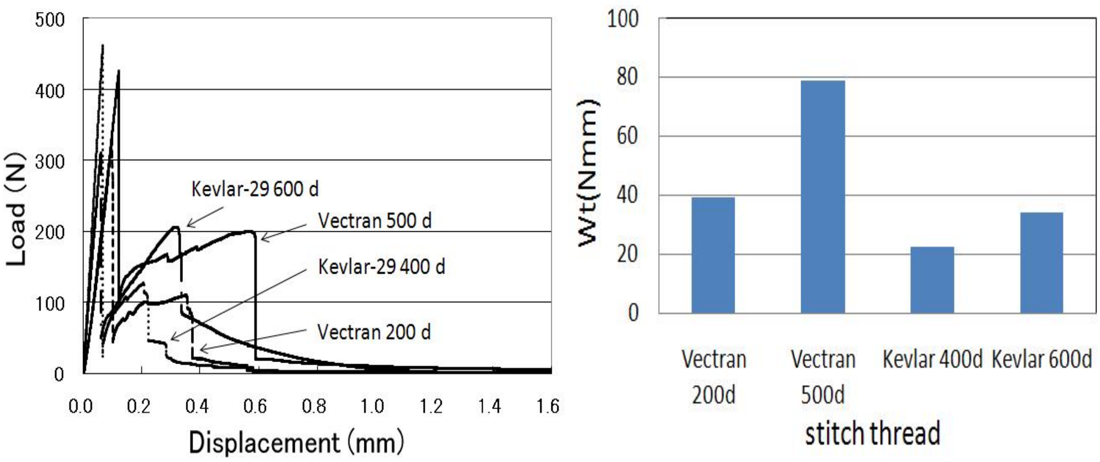

Figure 11. Vectran-Kevlar Comparison: ITT Results (left); Strain Energy (right)

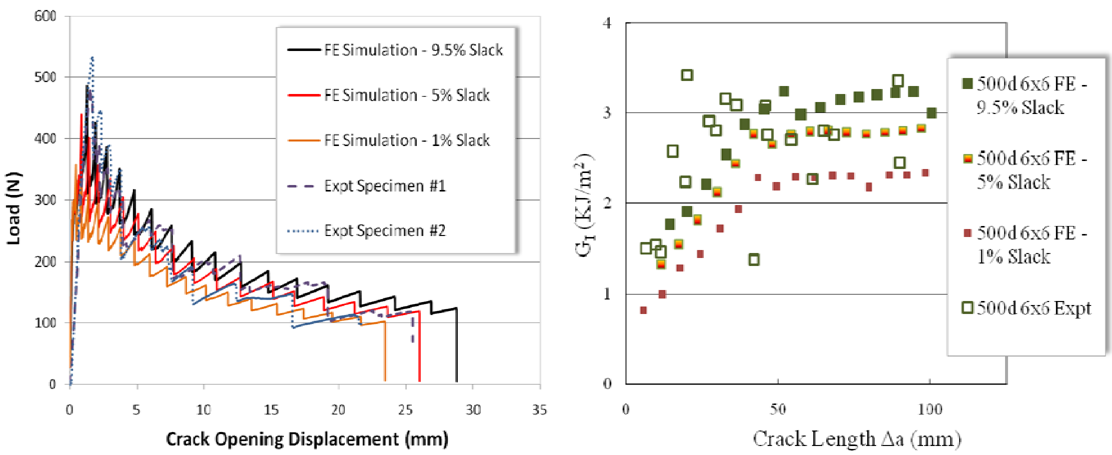

Figure 12. Effect of Slack Absorption on Vectran 500d 6x6 FE Simulation: Load-COD Curves (left); R-curves (right)

CONCLUSION

This paper confirms, by both experimental and analytical methods, that Z-fibre stitching has good effect on mode I interlaminar fracture toughness of laminated composites and the resistance to interlaminar fracture can be better improved by increasing stitch density and stitch thread thickness. DCB test and FE simulation are used to evaluate the interlaminar fracture toughness of laminated composites stitched with three different fibre materials – Carbon, Kevlar and Vectran. Vectran stitched composite exhibits 1.5 times higher G_I/SD value than Kevlar and Carbon stitched laminates of similar thread thickness. G_I/V_{ft} comparison reveals that Vectran fibre is more effective in interlaminar strengthening by 60%, compared with Kevlar and Carbon. This is due to consumption of higher strain energy and larger slack absorption during Vectran fibre breakage. It is concluded that Vectran is a better material choice for Z-fibre application.

ACKNOWLEDGEMENT

The authors would like to thank Tokyo Metropolitan Government (TMG) for its financial support from Asian Human Resources Fund under Project Asian Network for Major Cities 21 (ANMC 21).

References

1. Jain, L.K. and Mai, Y.W. (1994). Mode I Delamination Toughness of Laminated Composites with Through-Thickness Reinforcement, *Applied Composite Materials*, **1**: 1-17.

2. Dransfield, K.A., Jain, L.K. and Mai, Y.W. (1998). On the Effects of Stitching in CFRPs – I. Mode I Delamination Toughness, *Composites Science and Technology*, **58**: 815-827.

3. Tanzawa, Y., Watanabe, N. and Ishikawa, T. (1999). Interlaminar fracture toughness of 3-D orthogonal interlocked fabric composites, *Composites Science and Technology*, **59**: 1261-1270.

4. Tanzawa, Y., Watanabe, N. and Ishikawa, T. (2001). FEM simulation of a modified DCB test for 3-D orthogonal interlocked fabric composites, *Composites Science and Technology*, **61**: 1097-1107.

5. Mouritz, A.P. and Cox, B.N. (2000). A mechanistic approach to the properties of stitched laminates, *Composites: Part A*, **31**: 1-27.

6. Wood, M.D.K., Sun, X., Tong, L., Katzos, A., Rispler, A.R. and Mai, Y.W. (2007). The effect of stitch distribution on Mode I delamination toughness of stitched laminated composites – experimental results and FEA simulation, *Composites Science and Technology*, **67**: 1058-1072.

7. Iwahori, Y., Ishikawa, T., Watanabe, N., Ito, A., Hayashi, Y. and Sugimoto, S. (2007). Experimental investigation of interlaminar mechanical properties on carbon fiber stitched CFRP laminates, *Adv. Composite Mater.*, **16(2)**: 95-113.

8. Iwahori, Y., Nakane, K. and Watanabe, N. (2009). DCB Test Simulation of Stitched CFRP laminates using Interlaminar Tension Test Results, *Composites Science and Technology*, *in press*.